


Module-conditioned distribution of quantum circuits

Hyunho Cha ¹ and Jungwoo Lee ^{1*}

¹NextQuantum and Department of Electrical and Computer Engineering, Seoul National University, Seoul, 08826, Republic of Korea.

*Corresponding author(s). E-mail(s): junglee@snu.ac.kr;

Contributing authors: aiden132435@cml.snu.ac.kr;

Abstract

As quantum computers require highly specialized and stable environments to operate, expanding their capabilities within a single system presents significant technical challenges. By interconnecting multiple quantum processors, distributed quantum computing can facilitate the execution of more complex and larger-scale quantum algorithms. End-to-end heuristics for the distribution of quantum circuits have been developed so far. In this work, we derive an exact integer programming approach for the Distributed Quantum Circuit (DQC) problem, assuming fixed module allocations. Since every DQC algorithm necessarily yields a module allocation function, our formulation can be integrated with it as a post-processing step. This improves on the hypergraph partitioning formulation, which finds a module allocation function and an efficient distribution at once. We also show that a suboptimal heuristic to find good allocations can outperform previous methods. In particular, for quantum Fourier transform circuits, we conjecture from experiments that the optimal module allocation is the trivial one found by this method.

Keywords: Distributed quantum computing, Integer programming

Acknowledgments

This work is in part supported by the National Research Foundation of Korea (NRF, RS-2024-00451435 (20%), RS-2024-00413957 (40%)), Institute of Information & Communications Technology Planning & Evaluation (IITP, 2021-0-01059 (40%)), grant

funded by the Ministry of Science and ICT (MSIT), Institute of New Media and Communications (INMAC), and the Brain Korea 21 FOUR program of the Education and Research Program for Future ICT Pioneers.

1 Introduction

In recent years, the capacity of quantum computing hardware has steadily increased (Arute et al., 2019; Bravyi, Gosset, & König, 2018; Horowitz & Grumblin, 2019; Kjaergaard et al., 2020; Neill et al., 2018). However, a significant obstacle to realizing the full potential of quantum computing is the limited number of qubits available in a single quantum computer (or module) (Bourassa et al., 2021; Fowler, Mariantoni, Martinis, & Cleland, 2012; O’Malley et al., 2016; Terhal, 2015). To overcome this, distributing a large quantum computation over a network of modules has emerged as a promising approach (Cacciapuoti et al., 2019; Cirac, Ekert, Huelga, & Macchiavello, 1999; Cuomo et al., 2023; Eisert, Jacobs, Papadopoulos, & Plenio, 2000; Yimsiriwattana & Lomonaco Jr, 2004).

The Distributed Quantum Circuit (DQC) problem involves dividing a quantum circuit across multiple modules. A non-local controlled unitary gate between two modules can be realized from local operations if the modules share a Bell state (Nielsen & Chuang, 2010; Sych & Leuchs, 2009; Zaman, Jeong, & Shin, 2018), which is referred to as an *ebit* (Andres-Martinez et al., 2024; Andres-Martinez & Heunen, 2019; G Sundaram, Gupta, & Ramakrishnan, 2021; Wu et al., 2023). Typically, DQC attempts to minimize the ebit cost for circuit execution. Its goal is to map the qubits in the circuit to individual modules and determine how to implement the non-local operations in a way that minimizes the number of ebits and communications.

This paper primarily considers homogeneous networks with $k \geq 3$ modules. In this setting, distributions using a hypergraph partitioning formulation and heuristic solvers proved to be the most effective (Andres-Martinez et al., 2024; Wu et al., 2023). However, this approach jointly determines the module allocation and the implementation of non-local gates based on that allocation, even though the former cannot logically depend on the latter. As our main contribution, we observe that exact integer programming formulations (Karp, 2009; Papadimitriou & Steiglitz, 1998; Wolsey, 2020) yield improved ebit costs if the module allocation function is *fixed*, demonstrating stability for various types of circuits. First, we present formulations for $k \geq 4$ modules and then show how it simplifies for $k = 3$ modules. As a result, our method can be combined with any DQC solver by ignoring its distribution steps and adopting only the module allocation it returns. Our approach further reduces ebit costs for various types of circuits, with significant improvements observed in some structured circuits. This highlights the importance of our post-processing for achieving robust results.

We also propose a simple suboptimal heuristic to find a module allocation function, although we currently find it effective only for quantum Fourier transform (QFT) circuits (Coppersmith, 2002; Nielsen & Chuang, 2010; Ruiz-Perez & Garcia-Escartin, 2017). Interestingly, experimental results suggest that the proposed heuristic is likely to be optimal for these circuits.

The rest of this paper is organized as follows. Section 2 provides an overview of background and related works. In Section 3, we present detailed derivations and proofs of our binary integer programming (BIP) formulations, along with an explanation of the unique characteristics of distributing QFT circuits. Section 4 presents experimental results, which have been validated on various circuits. Finally, Section 5 concludes the paper and offers a perspective on future work.

2 Preliminaries

2.1 Distribution of quantum circuits

In the context of distributed quantum computing, a *module* refers to an individual quantum computer that forms part of a larger, interconnected network (Andres-Martinez et al., 2024).

As in previous studies, we consider a quantum circuit to be composed only of unary and binary gates (Andres-Martinez et al., 2024; Andres-Martinez & Heunen, 2019; G Sundaram et al., 2021; Wu et al., 2023). Here, each binary gate is a controlled-phase (*CP*) gate (Nielsen & Chuang, 2010)

$$CP(\theta) = |0\rangle\langle 0| \otimes \mathbb{I} + |1\rangle\langle 1| \otimes \begin{pmatrix} 1 & \\ & e^{i\theta} \end{pmatrix},$$

where \mathbb{I} denotes the single-qubit identity operator. Any circuit can be transformed into an equivalent circuit in this form, a fact that follows from the universality of the set consisting of all unary gates and the CNOT gate (Barenco et al., 1995).

Distributing an n -qubit quantum circuit involves two steps. First, each qubit must be assigned to a module. Second, non-local gates are identified based on this module allocation, and the optimal method to implement these gates with the least resources is determined. This overall process is referred to as the DQC problem. Typically, a (k, ϵ) *balanced partition* is used for module allocation, ensuring that each module contains at most $(1 + \epsilon)\frac{n}{k}$ qubits (G Sundaram et al., 2021). By a reduction from the hypergraph min-cut problem, the DQC problem was shown to be NP-hard (Andres-Martinez & Heunen, 2019).

2.2 Cat-entanglement & cat-disentanglement

A quantum communication channel enables the creation of the Bell state

$$\frac{|00\rangle_{AB} + |11\rangle_{AB}}{\sqrt{2}}$$

between two modules A and B , which is a maximally entangled bipartite state. In the context of DQC, such states are referred to as ebits. Fig. 1 shows how to implement a non-local controlled unitary gate with a single control qubit $|c\rangle$ and a single target qubit $|t\rangle$ at the cost of a single ebit. The steps before (after) the controlled unitary gate constitute a *cat-entanglement* (*cat-disentanglement*) process. The former creates a

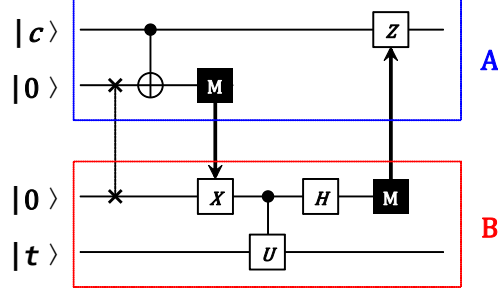


Fig. 1 A non-local controlled unitary gate can be realized using only local operations and classical communications at the cost of a single ebit.

linked copy of $|c\rangle$ in module B , and the latter effectively reverses this process. After cat-disentanglement, the operation $|ct\rangle \mapsto CP(\theta)|ct\rangle$ has been successfully implemented.

Suppose we create linked copies of a qubit q at modules other than the one including q . This cat-entanglement operation (a) commutes with CP gates acting on q and (b) generally does not commute with arbitrary unary gates acting on q (see appendices A & B). The first property allows us to restrict the creation of a linked copy of q in any module to occur immediately after one of the unary operations on q or at time 0, assuming that the circuit is compiled exclusively with CP gates and unary gates. The second property implies that in general, all linked copies of q in other modules must be reintegrated into q before a unary gate acts on q .

2.3 Problem formulation

We represent a quantum circuit acting on a set of n qubits $Q = \{q_i\}_{i=1}^n$ as a finite set $C = U \cup B$, where

$$U = \bigcup_{i=1}^n \left\{ (q_i, t) \mid t \in T^{(i)} \subset \mathbb{N} \right\}$$

is a set of unary gates and

$$B = \bigcup_{1 \leq i < j \leq n} \left\{ (\{q_i, q_j\}, t) \mid t \in T^{(\{i,j\})} \subset \mathbb{N} \right\}$$

is a set of *non-local* binary gates. As is clear from the notation, (q_i, t) represents a unary gate acting on q_i at time t and $(\{q_i, q_j\}, t)$ represents a binary gate acting on $\{q_i, q_j\}$ at time t . Without loss of generality, it is assumed that all $T^{(i)}$ and $T^{(\{i,j\})}$ are mutually exclusive.

In what follows, we assume that there are $k \geq 3$ modules in total, i.e., $P = \{p_1, p_2, \dots, p_k\}$, and that we are *given* a module allocation function $\pi : Q \rightarrow P$. This implies that $\pi(q_i) \neq \pi(q_j)$ for all $(\{q_i, q_j\}, t) \in B$. The concept of *migration* was first defined in Ref. (G Sundaram et al., 2021), which essentially represents the cat-entanglement operation in Section 2.2. It implicitly assumes that cat-disentanglements are performed whenever necessary.

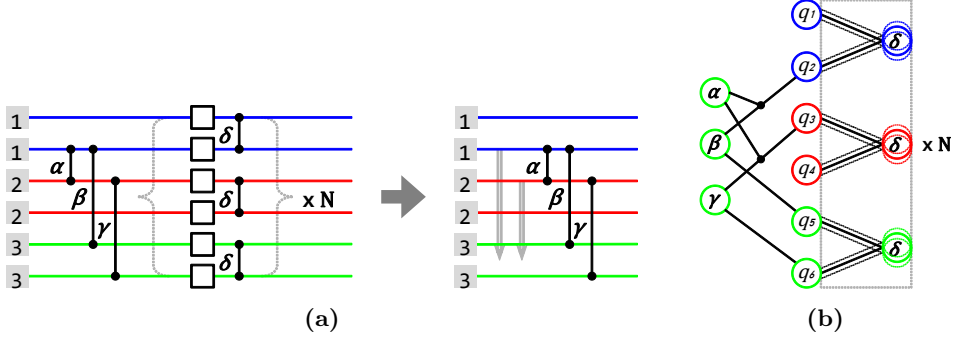


Fig. 2 (a) Distribution of a quantum circuit and (b) its hypergraph representation. Gray boxes represent module indices and gray arrows indicate migrations.

Definition 1 (Migration (G Sundaram et al., 2021)). A migration is a triple (q, p, t) , which translates to creating a linked copy of q in module p at time t . The set of all candidate migrations is defined as

$$M \equiv \bigcup_{i=1}^n \bigcup_{p \in P \setminus \{\pi(q_i)\}} \left\{ (q_i, p, t) \mid t \in \{0\} \cup T^{(i)} \right\}.$$

Definition 2 (Coverage (G Sundaram et al., 2021)). For a non-local CP gate $g = (\{q_i, q_j\}, t^*)$, we say that a migration (q, p, t) (see 1 & 2) or a pair of migrations $\{(q_{i'}, p, t), (q_{j'}, p, t')\}$ (see 3) covers g if one of the following conditions holds, thereby enabling the execution of g .

1. $q = q_i, p = \pi(q_j), t = \max_{\tilde{t} \in \{0\} \cup T^{(i)}, \tilde{t} \leq t^*} \tilde{t}$
2. $q = q_j, p = \pi(q_i), t = \max_{\tilde{t} \in \{0\} \cup T^{(j)}, \tilde{t} \leq t^*} \tilde{t}$
3. $\{i', j'\} = \{i, j\}, p \notin \{\pi(q_i), \pi(q_j)\},$
 $t = \max_{\tilde{t} \in \{0\} \cup T^{(i')}, \tilde{t} \leq t^*} \tilde{t}, t' = \max_{\tilde{t} \in \{0\} \cup T^{(j')}, \tilde{t} \leq t^*} \tilde{t}$

Given π , the problem of finding the minimum subset of M that covers all gates in B following Definition 2 is called *migration selection under general coverage* (MS-GC). If we do not allow 3 in Definition 2, then the problem is called *migration selection under home coverage* (MS-HC). An efficient optimal algorithm for MS-HC given π has been identified. On the other hand, MS-GC is conjectured to be NP-hard, and a heuristic was proposed, which greedily adds a set of migrations at each iteration based on some criterion (G Sundaram et al., 2021).

2.4 Hypergraph partitioning formulation

The problem of quantum circuit distribution can be reduced to a hypergraph partitioning problem (Andres-Martinez & Heunen, 2019), for which efficient heuristic solvers exist. This currently achieves the best results for $k \geq 3$ (Andres-Martinez et al., 2024;

Wu et al., 2023). Given a circuit C , the corresponding hypergraph is constructed as follows. First, a node is added for each binary gate and for each qubit. Second, for each qubit q_i and time interval $I = (t, t')$ such that the following conditions are satisfied, a hyperedge that connects q_i and all the binary gates that act on q_i within I is added, if such gate exists:

- $t, t' \in T^{(i)} \cup \{0, \infty\}, t < t'$
- $\{t'' \mid t'' \in T^{(i)}, t < t'' < t'\} = \emptyset$
- $\{(j, t'') \mid (\{q_i, q_j\}, t'') \in B, t < t'' < t'\} \neq \emptyset$

Fig. 2 shows an example circuit distributed by this method. The coverage of the gate α corresponds to 3 in Definition 2, and the coverages of the gates β and γ corresponds to 1 or 2 in Definition 2.

3 Main results

3.1 BIP formulation of MS-GC for $k \geq 4$

For notational simplicity, we define

$$f(i, t) \equiv \max \left(\{t' \in \{0\} \cup T^{(i)} \mid t' \leq t\} \right),$$

which denotes the latest time a unary gate is applied to q_i up to time t (or 0 if none exists). We define the following sets of migrations:

$$\begin{aligned} M^{(1, (\{q_i, q_j\}, t))} &\equiv \{(q_i, \pi(q_j), f(i, t)), \\ &\quad (q_j, \pi(q_i), f(j, t))\}, \\ M^{(2, (\{q_i, q_j\}, t))} &\equiv \{(q_i, p, f(i, t)), (q_j, p, f(j, t))\} \\ &\quad \mid p \in P \setminus \{\pi(q_i), \pi(q_j)\}\}. \end{aligned}$$

In simpler terms, $M^{(1, (\{q_i, q_j\}, t))}$ denotes a pair of migrations, where each migration in the pair migrates one of the qubits to the other qubit's module; $M^{(2, (\{q_i, q_j\}, t))}$ denotes a set of pairs of migrations, where each pair in the set comprises migrations that migrate both qubits to a module that contains neither of them. We proceed to define the following unions:

$$\begin{aligned} \tilde{M}^{(g)} &\equiv M^{(1, g)} \cup M^{(2, g)}, \\ M^{(1)} &\equiv \bigcup_{g \in B} M^{(1, g)}, \quad M^{(2)} \equiv \bigcup_{g \in B} M^{(2, g)}, \\ \tilde{M} &\equiv M \cup M^{(2)}. \end{aligned}$$

In order to describe a BIP formulation of MS-GC, we now view these *sets* as *lists* with indices as subscripts such that for any set S we can employ a slight abuse of notation:

$$\forall 1 \leq i \leq |S|, \quad S_i \in S \quad \text{and} \quad S.\text{idx}(S_i) = i.$$

Any ordering is acceptable as long as one remains consistent with it.

We begin by describing a BIP formulation of MS-GC for $k \geq 4$. A more efficient formulation for $k = 3$ is described in Section 3.2. Consider the binary matrix

$$A \in \{0, 1\}^{|B| \times |\tilde{M}|},$$

where

$$A_{ij} = \begin{cases} 1 & \text{if } \tilde{M}_j \in \tilde{M}^{(B_i)} \\ 0 & \text{otherwise} \end{cases}. \quad (1)$$

Each row of A contains $2 + (k - 2) = k$ non-zero elements. Let $x \in \{0, 1\}^{|\tilde{M}|}$ represent the set of all selected migrations and pairs of migrations, which is a subset of \tilde{M} . To ensure that x is a valid representation, we impose the constraint that if a pair of migration is selected, then each migration in the pair must also be selected. For each pair of migrations $\mathbf{m} \in M^{(2)}$, we add a constraint to the vector x as $e^{(\mathbf{m})\top} x \geq 0$, where

$$e^{(\mathbf{m})} \equiv e_{\tilde{M}.\text{idx}(\mathbf{m}_1)} + e_{\tilde{M}.\text{idx}(\mathbf{m}_2)} - 2e_{\tilde{M}.\text{idx}(\mathbf{m})}$$

and e_i denotes the i -th standard unit vector in $|\tilde{M}|$ dimensions.

Let $\mathbf{0}_d$ and $\mathbf{1}_d$ denote the all-zeros vector and the all-ones vector in d dimensions, respectively. Then the objective is defined as

$$\begin{aligned} & \text{minimize} \quad \left[\mathbf{1}_{|\tilde{M}|}^\top \mathbf{0}_{|M^{(2)}|}^\top \right] x \\ & \text{subject to} \quad \tilde{A}x \geq \left[\mathbf{1}_{|B|}^\top \mathbf{0}_{|M^{(2)}|}^\top \right]^\top, \end{aligned} \quad (2)$$

where

$$\tilde{A} \equiv \left[A^\top e^{(M_1^{(2)})} e^{(M_2^{(2)})} \dots e^{(M_{|M^{(2)}|}^{(2)})} \right]^\top$$

and A is defined as in (1) (see Algorithm 1). We explain the validity of this formulation through the following lemma.

Proposition 1. *A solution of (2) is an optimal solution of MS-GC.*

Proof. We show that it suffices to relax the constraint

$$x_{\tilde{M}.\text{idx}(\mathbf{m})} = x_{\tilde{M}.\text{idx}(\mathbf{m}_1)} x_{\tilde{M}.\text{idx}(\mathbf{m}_2)} \quad (3)$$

to

$$x_{\tilde{M}.\text{idx}(\mathbf{m})} \leq x_{\tilde{M}.\text{idx}(\mathbf{m}_1)} x_{\tilde{M}.\text{idx}(\mathbf{m}_2)}. \quad (4)$$

Since x is a binary vector, (4) is equivalent to

$$\begin{aligned} x_{\tilde{M}.\text{idx}(\mathbf{m}_1)} - x_{\tilde{M}.\text{idx}(\mathbf{m})} &\geq 0, \\ x_{\tilde{M}.\text{idx}(\mathbf{m}_2)} - x_{\tilde{M}.\text{idx}(\mathbf{m})} &\geq 0, \end{aligned} \quad (5)$$

Table 1 Truth table for (5) & (6).

$x_{\tilde{M}.\text{idx}(\mathbf{m}_1)}$	$x_{\tilde{M}.\text{idx}(\mathbf{m}_2)}$	$x_{\tilde{M}.\text{idx}(\mathbf{m})}$	(5)	(6)
0	0	0	T	T
0	0	1	F	F
0	1	0	T	T
0	1	1	F	F
1	0	0	T	T
1	0	1	F	F
1	1	0	T	T
1	1	1	T	T

and these two constraints can be merged into a single constraint as

$$x_{\tilde{M}.\text{idx}(\mathbf{m}_1)} + x_{\tilde{M}.\text{idx}(\mathbf{m}_2)} - 2x_{\tilde{M}.\text{idx}(\mathbf{m})} \geq 0, \quad (6)$$

reducing the number of constraints by half. The equivalence of (5) and (6) is verified in Table 1.

Algorithm 1 BIP for MS-GC, $k \geq 4$

```

1: Input: Unary gates  $U$ , binary gates  $B$ , module allocation function  $\pi$ 
2: Output: Vector of selected migrations  $x$ 
3: Initialize:
4:    $v^\top \leftarrow \begin{bmatrix} \mathbf{1}_{|M|}^\top & \mathbf{0}_{|M^{(2)}|}^\top \end{bmatrix}$ 
5:    $\tilde{A} \in \mathbb{B}^{(|B|+|M^{(2)}|) \times |\tilde{M}|} \leftarrow 0$ 
6:    $b^\top \leftarrow \begin{bmatrix} \mathbf{1}_{|B|}^\top & \mathbf{0}_{|M^{(2)}|}^\top \end{bmatrix}$ 
7: for  $j = 1$  to  $|\tilde{M}|$  do
8:   for  $i = 1$  to  $|B|$  do
9:     if  $\tilde{M}_j \in \tilde{M}^{(B_i)}$  then
10:       $\tilde{A}_{ij} \leftarrow 1$ 
11:     end if
12:   end for
13:   for  $i = 1$  to  $|M^{(2)}|$  do
14:     if  $\tilde{M}_j \in M_i^{(2)}$  then
15:       $\tilde{A}_{(|B|+i)j} \leftarrow 1$ 
16:     else if  $\tilde{M}_j = M_i^{(2)}$  then
17:       $\tilde{A}_{(|B|+i)j} \leftarrow -2$ 
18:     end if
19:   end for
20: end for
21: Solve BIP for  $x \in \mathbb{B}^{|\tilde{M}|}$ :
22:   Minimize  $v^\top x$  subject to  $\tilde{A}x \geq b$ .
23: return  $x$ 

```

The only combination that violates (3) while making (6) true is

$$\left(x_{\tilde{M}.\text{idx}(\mathbf{m}_1)}, x_{\tilde{M}.\text{idx}(\mathbf{m}_2)}, x_{\tilde{M}.\text{idx}(\mathbf{m})}\right) = (1, 1, 0).$$

However, it is easy to see that this does not disturb the formulation. Let \hat{x} be an optimal solution of (2) and assume that

$$\hat{x}_{\tilde{M}.\text{idx}(\mathbf{m}_1)} = \hat{x}_{\tilde{M}.\text{idx}(\mathbf{m}_2)} = 1, \quad \hat{x}_{\tilde{M}.\text{idx}(\mathbf{m})} = 0$$

for some $\mathbf{m} \in M^{(2)}$. Then $\hat{x}^{(\mathbf{m})} \equiv \hat{x} + e_{\tilde{M}.\text{idx}(\mathbf{m})}$ is also an optimal solution because

$$\begin{bmatrix} \mathbf{1}_{|M|}^\top & \mathbf{0}_{|M^{(2)}|}^\top \end{bmatrix} \hat{x}^{(\mathbf{m})} = \begin{bmatrix} \mathbf{1}_{|M|}^\top & \mathbf{0}_{|M^{(2)}|}^\top \end{bmatrix} \hat{x}$$

and

$$\begin{aligned} \tilde{A}\hat{x}^{(\mathbf{m})} &= \tilde{A}\hat{x} + \tilde{A}e_{\tilde{M}.\text{idx}(\mathbf{m})} \\ &\geq \tilde{A}\hat{x} = \begin{bmatrix} \mathbf{1}_{|B|}^\top & \mathbf{0}_{|M^{(2)}|}^\top \end{bmatrix}^\top, \end{aligned}$$

i.e., $\hat{x}^{(\mathbf{m})}$ is also an optimal solution of (2), which satisfies (3). \square

Algorithm 2 BIP for MS-GC, $k = 3$

```

1: Input: Unary gates  $U$ , binary gates  $B$ , module allocation function  $\pi$ 
2: Output: Vector of selected migrations  $x$ 
3: Initialize:
4:    $v^\top \leftarrow \mathbf{1}_{|M^{(1)}|}^\top$ 
5:    $A \in \mathbb{B}^{|B| \times |M^{(1)}|} \leftarrow 0$ 
6:    $b \leftarrow 2 \cdot \mathbf{1}_{|B|}$ 
7: for  $i = 1$  to  $|B|$  do
8:   for  $j = 1$  to  $|M^{(1)}|$  do
9:     if  $M_j^{(1)} \in M^{(1, B_i)}$  then
10:       $A_{ij} \leftarrow 2$ 
11:     else if  $M_j^{(1)} \in M_1^{(2, B_i)}$  then
12:       $A_{ij} \leftarrow 1$ 
13:     end if
14:   end for
15: end for
16: Solve BIP for  $x \in \mathbb{B}^{|M^{(1)}|}$ :
17:   Minimize  $v^\top x$  subject to  $Ax \geq b$ .
18: return  $x$ 

```

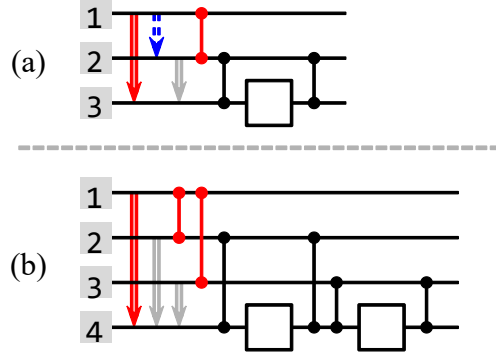


Fig. 3 Gray boxes represent module indices. (a) Removing the red migration leaves the red gate uncovered, which is covered by the blue migration. (b) Removing the red migration leaves the red gates uncovered, which is *not* covered by any single migration.

3.2 BIP formulation of MS-GC for $k = 3$

If $k = 3$, we observe that the number of BIP variables and constraints can be further reduced. Consider the matrix

$$A \in \mathbb{B}^{|B| \times |M^{(1)}|},$$

where

$$A_{ij} = \begin{cases} 2 & \text{if } M_j^{(1)} \in M^{(1, B_i)} \\ 1 & \text{if } M_j^{(1)} \in M_1^{(2, B_i)} \\ 0 & \text{otherwise} \end{cases} \quad (7)$$

(see Algorithm 2). To avoid confusion, notice that

$$M_1^{(2, g)} = \{(q_i, p, f(i, t)), (q_j, p, f(j, t))\},$$

where $g = (\{q_i, q_j\}, t)$ and $p \in P \setminus \{\pi(q_i), \pi(q_j)\}$ is unique. Before we describe the objective function, we remark that the optimization is respect to $x \in \mathbb{B}^{|M^{(1)}|}$ instead of $x \in \mathbb{B}^{|M|}$. We justify this reduction of variables through the following lemma.

Lemma 1. *If $k = 3$, the power set $2^{M^{(1)}}$ includes an optimal choice of migrations.*

Proof. We prove by contradiction. Let $P = \{p_1, p_2, p_3\}$ and $\pi(q_i) = p_1$. Suppose $m = (q_i, p_2, t) \notin M^{(1)}$ for some $m \in M$ is strictly necessary. By the definition of $M^{(1)}$, there is no gate $(\{q_i, q_j\}, t')$ such that $\pi(q_j) = p_2$ and $f(i, t') = t$. This means that the non-local binary gates that m can cover (by itself or in a pair with another migration) must be in the form of $(\{q_i, q_j\}, t')$, where $\pi(q_j) = p_3$ and $f(i, t') = t$ (and in fact, m cannot cover one of these gates by itself because it migrates q_i in p_1 to p_2 while the gate acts on a qubit in p_3 ; it must be paired with a migration that sends q_j to p_2). Since we assumed that m is strictly necessary, there must exist at least one such gate. Meanwhile, notice that those gates are all covered by the *single* migration $m' = (q_i, p_3, t) \in M^{(1)}$. Therefore, replacing m with m' does not increase the number

of selected migrations without introducing any uncovered gates, which implies that any migration $m \notin M^{(1)}$ is not strictly necessary; each of them can be replaced by some $m' \in M^{(1)}$. \square

Fig. 3 provides an example circuit to visualize Lemma 1, as well as a circuit with $k = 4$ to which the lemma does not apply.

The objective is defined as

$$\begin{aligned} & \text{minimize} && \mathbf{1}_{|M^{(1)}|}^\top x \\ & \text{subject to} && Ax \geq 2 \cdot \mathbf{1}_{|B|}, \end{aligned} \tag{8}$$

where A is defined as in (7). We explain the validity of this formulation through the following lemma.

Proposition 2. *A solution of (8) is an optimal solution of MS-GC for $k = 3$.*

Proof. By the definition of A , it is clear that $A_{i,:}x \geq 2$ if and only if a non-empty subset of $\{M_1^{(1,B_i)}, M_2^{(1,B_i)}, M_1^{(2,B_i)}\}$ is selected, where $A_{i,:}$ denotes the i -th row of A . \square

Note that this is not a valid formulation for $k \geq 4$. For a gate $g = (\{q_i, q_j\}, t)$, consider two modules $p, p' \in P \setminus \{\pi(q_i), \pi(q_j)\}$ such that $p \neq p'$. We cannot distinguish the selection of the pair

$$\{(q_i, p, f(i, t)), (q_j, p, f(j, t))\}$$

which covers g from the pair

$$\{(q_i, p, f(i, t)), (q_j, p', f(j, t))\}$$

which does not cover g . In general, it is impossible for four positive ‘rewards’ r_1, r_2, r_3 , and r_4 to satisfy the conditions where $r_1 + r_2$ and $r_3 + r_4$ are greater than or equal to a threshold th , while $r_1 + r_3, r_1 + r_4, r_2 + r_3$, and $r_2 + r_4$ are all less than th .

3.3 Examples and analysis

Fig. 4 shows an example circuit distributed by the hypergraph partitioning formulation introduced in Section 2.4 and the BIP formulation described in this section. Even for these small circuits, the hypergraph partitioner begins to find suboptimal solutions, and the BIP post-processing helps reduce the ebit cost.

Assuming that there are at least $O(n)$ gates in C , the number of binary variables is

$$\begin{aligned} |M| + |M^{(2)}| &\leq (k-1)(|U| + n) + (k-2)|B| \\ &= O(k|C|) \end{aligned}$$

for (2) and

$$|M^{(1)}| \leq 2|B|$$

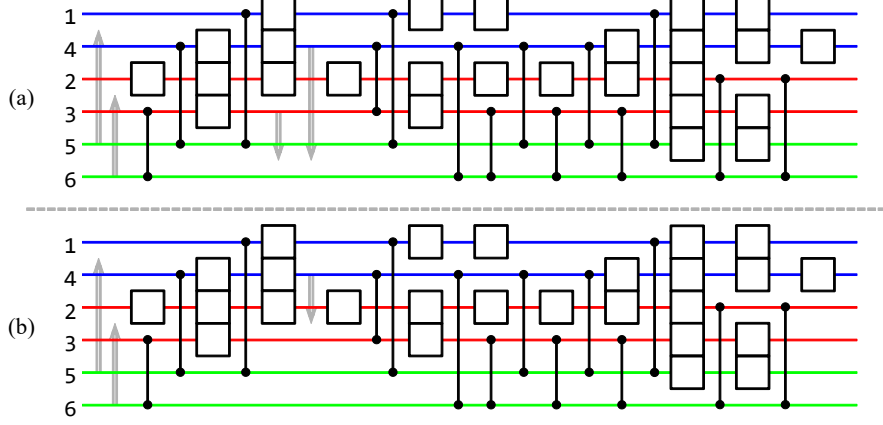


Fig. 4 (a) Distribution found by a hypergraph partitioner and (b) module-conditioned BIP. Numbers denote qubit indices and wires of the same color are assigned to the same module.

for (8). Also, the number of constraints is

$$|B| + |M^{(2)}| \leq (k - 1)|B|$$

for (2) and $|B|$ for (8).

Remark 1. The BIP formulations (2) and (8) is naturally generalized to heterogeneous settings, where the communication cost between each pair of modules is not constant. We simply replace $\begin{bmatrix} \mathbf{1}_{|M|}^\top & \mathbf{0}_{|M^{(2)}|}^\top \end{bmatrix}$ and $\mathbf{1}_{|M^{(1)}|}^\top$ with the vectors that represent the cost function.

3.4 Partitioning QFT

In Section 3, we have discussed the suboptimality of Ref. (Andres-Martinez & Heunen, 2019) for MS-GC given a module allocation function π . Meanwhile, we observe that it also returns suboptimal module allocation functions (recall that the hypergraph partitioning formulation finds π and selects migrations at once).

Assuming an arbitrary module allocation and MS-GC, finding an optimal π for a given circuit is generally a hard problem. Here, we explain a very specific case that can be solved easily. That is, assuming a balanced module allocation and MS-HC, we can find an optimal π for a QFT circuit.

Definition 3. A (k, m) -balanced distribution of QFT is a distribution of the QFT circuit for $n = km$ qubits, where k and m denote the number of modules and the number of qubits per module, respectively.

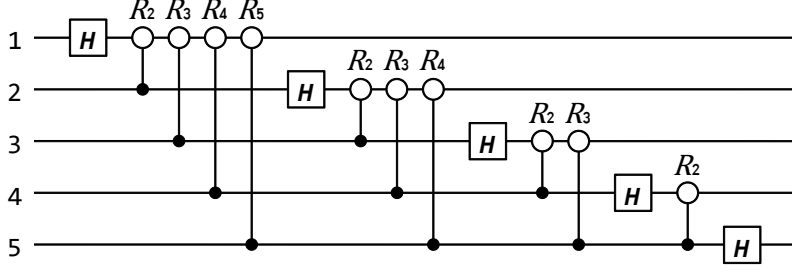


Fig. 5 5-qubit QFT circuit (SWAP gates omitted).

The basic structure of QFT before distribution is shown in Fig. 5. It consists of the Hadamard gates H and CP gates

$$CP(2\pi/2^k) = |0\rangle\langle 0| \otimes \mathbb{I} + |1\rangle\langle 1| \otimes R_k.$$

Note that we can omit the final SWAP gates and interpret the qubits in reverse order (Ruiz-Perez & Garcia-Escartin, 2017; Weinstein, Pravia, Fortunato, Lloyd, & Cory, 2001). In the subsequent diagrams, we replace each $H/CP(2\pi/2^k)$ gate with a general unary/ CP gate symbol.

It turns out that we can derive an optimal solution for any (k, m) -balanced distribution of QFT, assuming MS-HC.

Lemma 2. *The minimum ebit cost for a (k, m) -balanced distribution of the QFT circuit for $n = km$ qubits with MS-HC is $m \binom{k}{2}$.*

Proof. We provide a simple constructive proof. The QFT circuit for $n = km$ qubits can be fully described by the sets

$$U = \{(q_i, t_{q_i})\}_{i=1}^n$$

and

$$\tilde{B} = \{(\{q_i, q_j\}, t_{\{q_i, q_j\}})\}_{1 \leq i < j \leq n},$$

because the circuit includes only one unary gate per qubit and one binary gate per pair of qubits. That is, t_{q_i} and $t_{\{q_i, q_j\}}$ are uniquely defined. Assume that the qubits and gates are arranged in the conventional order as shown in Fig. 5 and let π be a balanced module allocator function, i.e.,

$$|\{i | \pi(q_i) = p_\kappa\}| = m, \quad \forall \kappa \in \{1, 2, \dots, k\}.$$

Consider a migration (q, p, t) where $\pi(q) \neq p$, and let S be the set of non-local binary gates that can be covered by this migration. Since we assume MS-HC, S is a subset of

$$\left\{ (\{q_i, q_j\}, t_{\{q_i, q_j\}}) \mid (q, p) \in \{(q_i, \pi(q_j)), (q_j, \pi(q_i))\} \right\},$$

which is equal to

$$\{(\{q, q'\}, t_{\{q, q'\}}) \mid \pi(q') = p\},$$

so $|S| \leq m$. Meanwhile, the total number of non-local binary gates in the distributed circuit is

$$\begin{aligned} \# \text{ binary} - \# \text{ local binary} &= \binom{n}{2} - k \binom{m}{2} \\ &= \frac{km(km-1)}{2} - k \frac{m(m-1)}{2} \\ &= \frac{k(k-1)m^2}{2}. \end{aligned}$$

This gives a lower bound on the ebit cost:

$$\frac{k(k-1)m^2}{2m} = \frac{k(k-1)m}{2}. \quad (9)$$

Now take $\pi = \pi^*$, where the *canonical partition* π^* is defined as

$$\pi^*(q_i) = p_{\lceil i/m \rceil}. \quad (10)$$

Then the set of all non-local binary gates is

$$B = \bigcup_{i=1}^{(k-1)m} \bigcup_{\kappa=\lceil i/m \rceil+1}^k \left\{ (\{q_i, q_j\}, t_{\{q_i, q_j\}}) \mid \lceil j/m \rceil = \kappa \right\} \quad (11)$$

and the circuit do distribute is $C = U \cup B$. But each $(\{q_i, q_j\}, t_{\{q_i, q_j\}})$ in (11) is covered by

$$(q_i, p_{\lceil j/m \rceil}, f(i, t_{\{q_i, q_j\}}) = t_{q_i}),$$

and it follows that the set

$$\{(q_i, p_\kappa, t_{q_i}) \mid \lceil i/m \rceil < \kappa \leq k\}$$

covers all gates in B with ebit cost $k(k-1)m/2$, which achieves its lower bound (9). \square

Note that π^* in Lemma 2 is not the only optimal module allocation for MS-HC (see Fig. 6). However, for $(k, m) = (3, 2)$, it is very likely that π^* is the only optimal module allocation for MS-GC (see Table 2). We also ran exhaustive experiments to find the optimal allocations among all balanced allocations for $(k, m) = (4, 2)$ and $(k, m) = (3, 3)$ (see Fig. 7). In both cases, the canonical partitions π^* were optimal for MS-GC (assuming that the BIP solver found optimal solutions for these small examples). That is, distributing a QFT circuit by solving the BIP associated with π^*

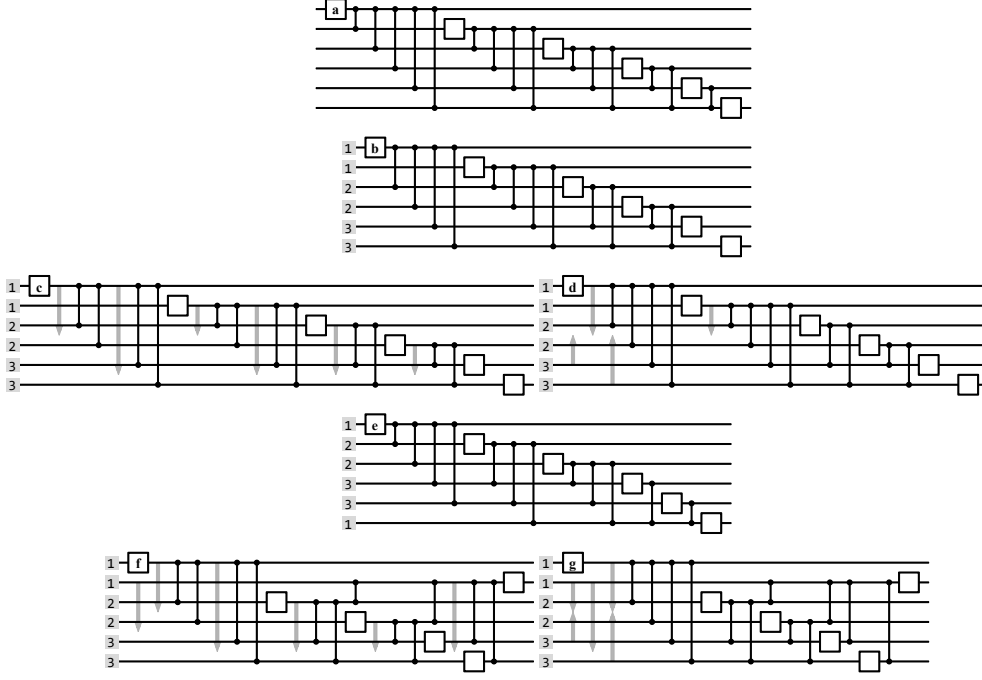


Fig. 6 (a) A 6-qubit QFT circuit. (b–d) Circuit C , MS-HC, and MS-GC for module allocation ‘112233’. (e–g) Circuit C , MS-HC, and MS-GC for module allocation ‘122331’. Both (c) and (f) involve 6 migrations, which is optimal for MS-HC. However, (d) involves 4 migrations while (g) involves 5 migrations for MS-GC.

is expected to yield the lowest ebit cost we can hope for. Indeed, we observe that this heuristic proves effective (see Section 4.2.1).

Remark 2. *One might be tempted to apply this heuristic to general circuits, i.e., finding an optimal π for MS-HC and solving the associated BIP for MS-GC. Unfortunately, this approach appears impractical at present because in general, it is unlikely that we can find an optimal π even for MS-HC. Also, there is no guarantee that an optimal π for MS-HC is also optimal for MS-GC.*

4 Experiments

The same algorithm and configuration described in Ref. (Andres-Martinez et al., 2024) were used for hypergraph partitioning. For the BIP solver, we used Gurobi 11.0.0 with a Named-User Academic License (Gurobi Optimization, LLC, 2024). It is based on the *branch-and-bound* paradigm for discrete optimization problems (Clausen, 1999; Land & Doig, 2009). We outline the types of circuits considered in our experiments and show the results. In all the following examples, *every* single run of the BIP solver resulted in

π	ebit cost	π	ebit cost
112233	4	112323	5
112332	5	121233	5
121323	6	121332	6
122133	5	123123	6
123132	6	122313	6
123213	6	123312	6
122331	5	123231	6
123321	6	—	—

Table 2 Module allocations and ebit costs found by BIP for $(3, 2)$ -balanced distributions of QFT.

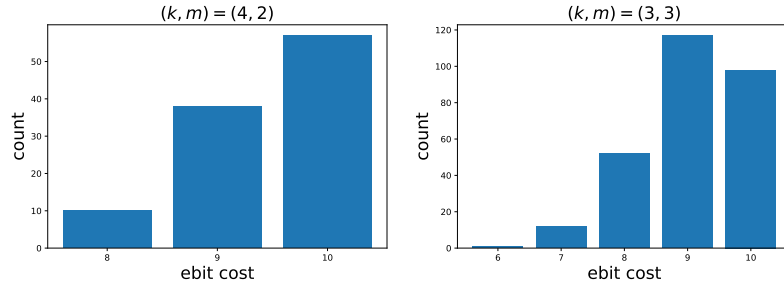


Fig. 7 Histograms of ebit cost for QFT circuits. Height indicates the number of allocations.

an ebit cost less than or equal to the non-post-processed case, demonstrating stability and general applicability of our approach.

4.1 Random circuits

4.1.1 CZ fraction circuits

Given parameters (n, d, p) , an n -qubit CZ fraction circuit is generated as described in Algorithm 3 (G Sundaram et al., 2021). Fig. 8 shows an example CZ fraction circuit. In all plots, ‘HP’ stands for the hypergraph partitioning solution. Ebit costs for distributing random CZ fraction circuits are shown in Fig. 9.

4.1.2 Quantum volume circuits

Given parameters (n, d) , an n -qubit quantum volume circuit is generated as described in Algorithm 4 (Cross, Bishop, Sheldon, Nation, & Gambetta, 2019). Fig. 10 (right) shows an example quantum volume circuit. Ebit costs for distributing random quantum volume circuits are shown in Fig. 11.

Algorithm 3 *CZ fraction*

```
1: Input:  $n, d, p$ 
2: Output: A random  $n$ -qubit circuit
3: Initialize:
4:    $U \leftarrow \emptyset$ 
5:    $B \leftarrow \emptyset$ 
6: for  $l = 1$  to  $d$  do
7:   for  $i = 1$  to  $n$  do
8:     With probability  $1 - p$ , add a unary gate acting on  $q_i$  to  $U$ .
9:   end for
10:  Randomly pair the qubits to which no unary gate was applied and add a CZ
    gate to  $B$  for each pair.
11: end for
12: return  $C = U \cup B$ 
```

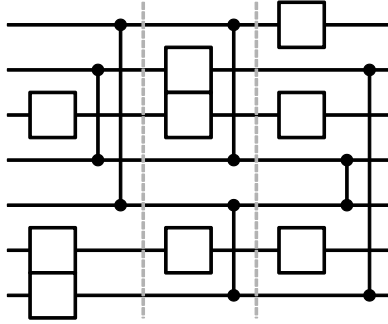


Fig. 8 An example 7-qubit 3-layer *CZ* fraction circuit with $p = 4/7$.

Algorithm 4 Quantum volume

```
1: Input:  $n, d$ 
2: Output: A random  $n$ -qubit circuit
3: for  $l = 1$  to  $d$  do
4:   Split  $Q$  into  $\lfloor n/2 \rfloor$  pairs  $\{\{q_i, q'_i\}\}_{1 \leq i \leq \lfloor n/2 \rfloor}$ .
5:   for  $i = 1$  to  $\lfloor n/2 \rfloor$  do
6:     Generate a random unitary from  $SU(4)$  according to the Haar measure and
       apply it to  $\{q_i, q'_i\}$ .
7:   end for
8: end for
9: Transpile the resulting circuit to unary gates  $U$  and  $CP$  gates  $B$ .
10: return  $C = U \cup B$ 
```

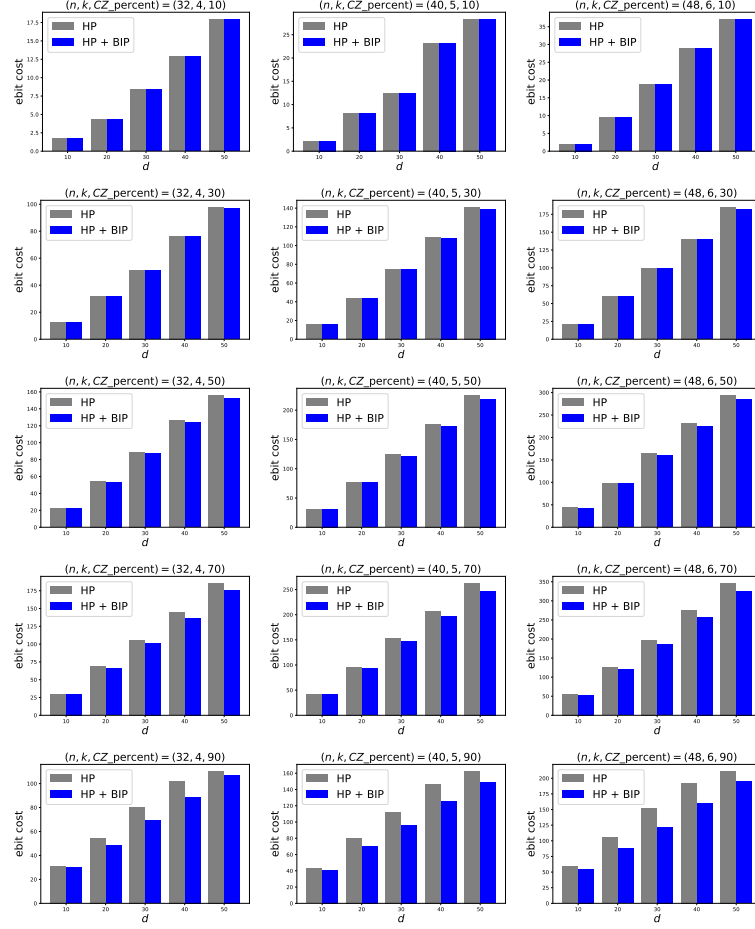


Fig. 9 BIP improvements observed in CZ fraction circuits. The reduction in ebit cost generally increases with higher CZ fractions, since they correspond to more difficult DQC instances.

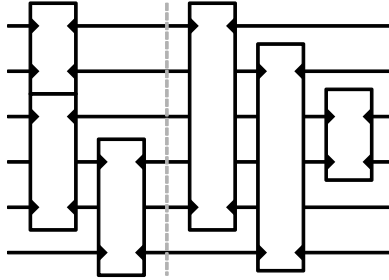


Fig. 10 An example 6-qubit 2-layer quantum volume circuit before transpilation.

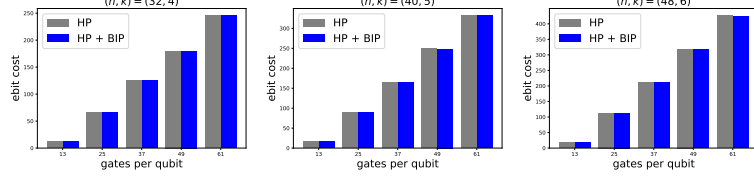


Fig. 11 BIP improvements observed in quantum volume circuits. The reduction in ebit cost is relatively marginal for these circuits. This is because as mentioned in (Andres-Martinez et al., 2024), rewriting a given quantum volume circuit such that all non-unary gates are CP gates makes the fraction of binary gates quite low. Similar to the results for circuits with low $CZ_percent$ shown in Fig. 9, little improvement is expected.

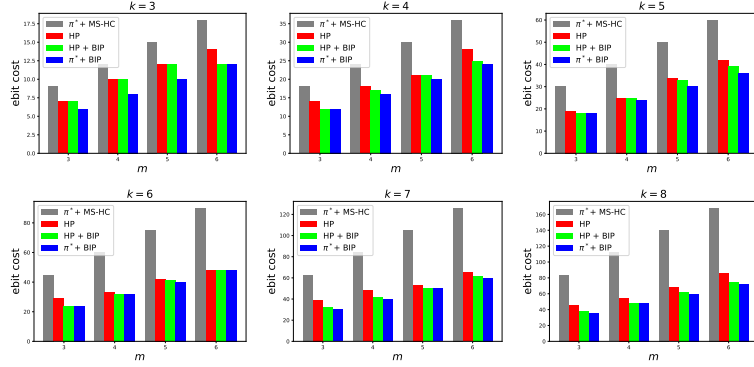


Fig. 12 BIP and/or π^* improvements observed in QFT circuits.

4.2 Arithmetic circuits

4.2.1 QFT circuits

Ebit costs for distributing QFT circuits are shown in Fig. 12. We remark that replacing π (found by a hypergraph partitioner) with π^* defined in (10) improved the ebit cost in every single run of the BIP solver. In this regard, we conjecture that for the distribution of QFT circuits, π^* is not only the optimal module allocation function for MS-HC but also for MS-GC.

4.2.2 DraperQFTAdder

The DraperQFTAdder is a quantum circuit that leverages QFT to perform addition (Draper, 2000). Before distribution, we perform a minor optimization on this circuit. Consider the identity

$$CP_{12}(\theta) = \text{SWAP}_{23} CP_{13}(\theta) \text{SWAP}_{23}, \quad (12)$$

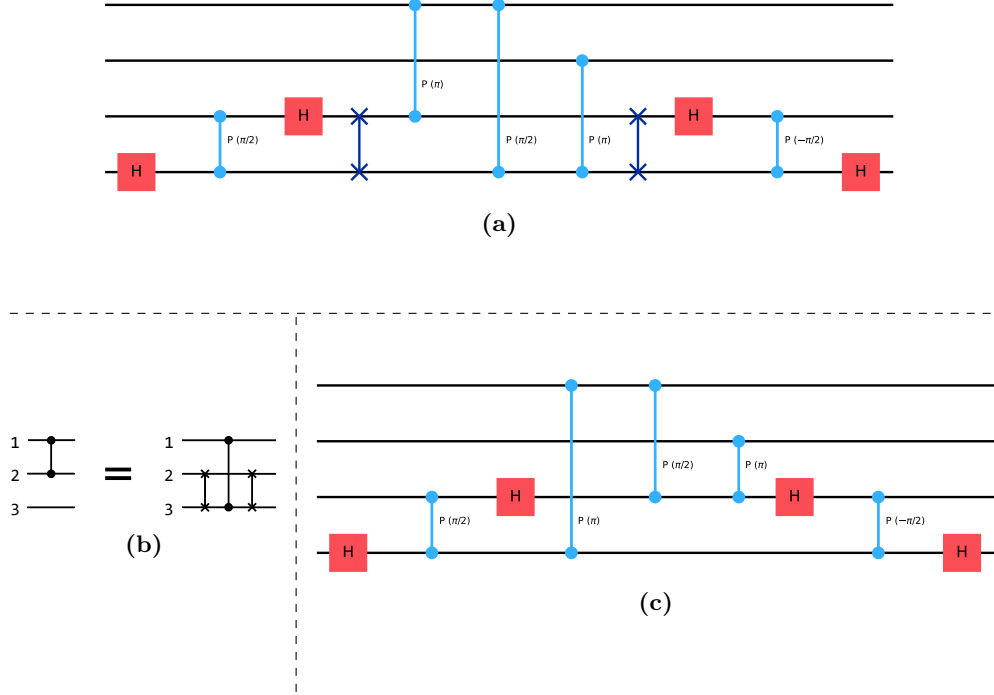


Fig. 13 (a) Example DraperQFTAdder circuit that performs in-place addition (modulo 2^2) on two 2-qubit registers. (b) Circuit representation of (12). (c) Equivalent circuit obtained by applying (12).

where the subscripts denote qubit indices (see APPENDIX C). The right-hand side appears many times in DraperQFTAdder circuits (Fig. 13). Since SWAP gates require binary gates to implement, we replace the right-hand side of (12) with the left-hand side. Ebit costs for distributing DraperQFTAdder circuits are shown in Fig. 14.

4.2.3 RGQFTMultiplier

The RGQFTMultiplier is a quantum circuit that leverages QFT to perform multiplication (Ruiz-Perez & Garcia-Escartin, 2017). They store the product of two n' -bit inputs out-of-place. By default, the output register has $2n'$ qubits, resulting in a total of $4n'$ qubits (Fig. 15).

Ebit costs for distributing RGQFTMultiplier circuits are shown in Fig. 16. Surprisingly, the hypergraph partitioner alone returns extremely inefficient distributions in many cases; post-processing with the BIP solver reduces the ebit costs significantly.

4.3 Boolean logic circuits

The hypergraph partitioning approach performs well for random circuits but sometimes fails to yield good solutions for circuits with fixed structures, as observed in the

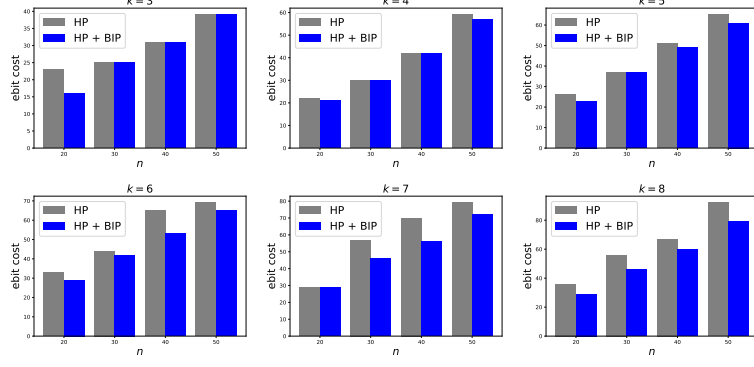


Fig. 14 BIP improvements observed in DraperQFTAdder circuits.

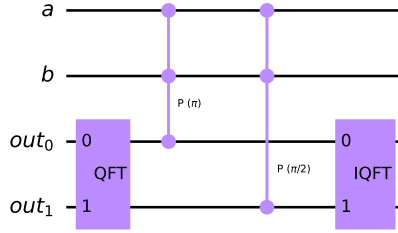


Fig. 15 Example RGQFTMultiplier circuit that computes the product of two bits ($n' = 1$).

case of RGQFTMultiplier. Unfortunately, we have yet to identify the reasons behind this failure.

The BIP post-processing based on a given module allocation function (found by any means) enhances stability. We present two additional examples of Boolean logic circuits: the AND circuit and the InnerProduct circuit. Even for small circuit size parameters, the impact of BIP post-processing is significant.

4.3.1 AND circuits

The AND circuit implements the logical AND operation on a number of qubits, i.e., it is a multi-controlled X gate (Fig. 17a). Ebit costs for distributing AND circuits are shown in Fig. 18.

4.3.2 InnerProduct circuits

InnerProduct is a $2n$ -qubit Boolean function that computes the inner product of two n -qubit vectors over F_2 (Fig. 17b):

$$\mathcal{IP}_{2n}(x_1, \dots, x_n, y_1, \dots, y_n) = (-1)^{x \cdot y}.$$

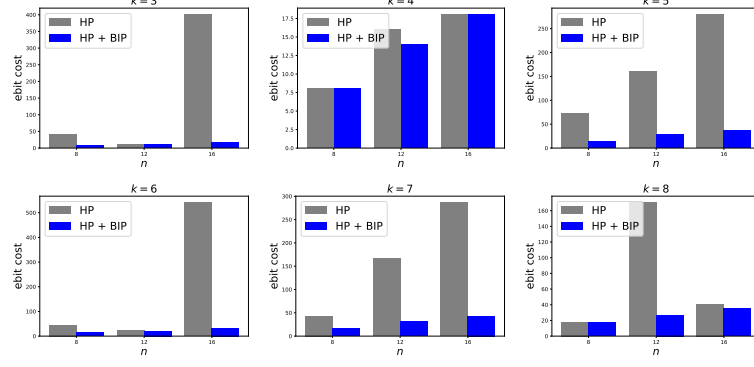


Fig. 16 BIP improvements observed in RGQFTMultiplier circuits.

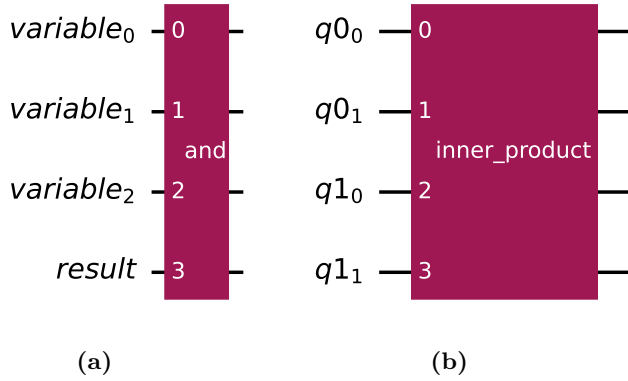


Fig. 17 (a) Example logical AND operation on 3 qubits. (b) Example 4-qubit Boolean function that computes the inner product of two 2-qubit vectors over F_2 .

Ebit costs for distributing InnerProduct circuits are shown in Fig. 19.

5 Conclusion and outlook

In this work, we proposed BIP formulations for the distribution of quantum circuits with fixed module allocation function. We take the module allocation returned by the hypergraph partitioning formulation of DQC, which had previously achieved the best results for $k \geq 3$ modules. Combining our post-processing step with existing methods for module allocation yields new best results. We also show that the problem can be further optimized for $k = 3$ by leveraging the unique properties of this specific case.

As is typical for DQC, our method is applicable to any quantum circuits constructed exclusively with unary gates and CP gates. Of these, QFT circuits have been found to reveal special properties in experiments. That is, taking the conventional

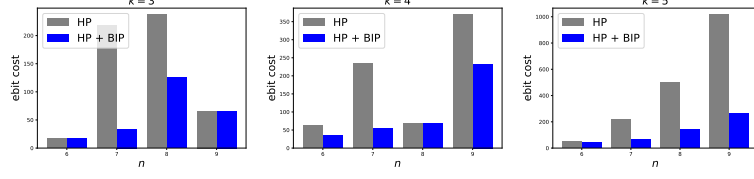


Fig. 18 BIP improvements observed in AND circuits.

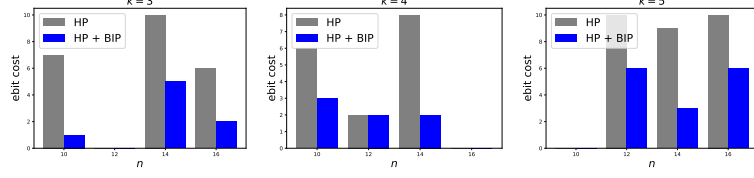


Fig. 19 BIP improvements observed in InnerProduct circuits. Empty bars indicate zero ebit cost.

ordering of qubits as the module allocation is optimal for MS-HC. Based on numerical results, we further conjecture that this module allocation is also optimal for MS-GC.

We believe that for many practical circuits, observing local properties may enable further reduction in the number of BIP variables and/or constraints. Identifying these properties is a promising future research direction to enhance the scalability of our approach. We also look forward to developing integer programming models for other circuit distribution protocols beyond the cat-entanglement-based approach and/or addressing connectivity between modules (Ferrari, Carretta, & Amoretti, 2023).

Appendix A Cat-entanglements commute with CP gates

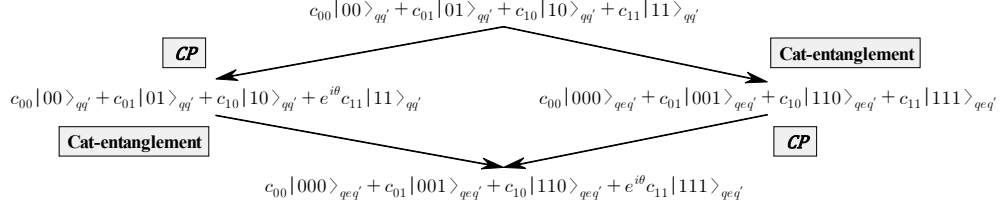


Fig. 20 A linked copy e of q is created at the module containing q' . The order of cat-entanglement and CP does not matter.

Appendix B Cat-entanglements do not commute with unary gates

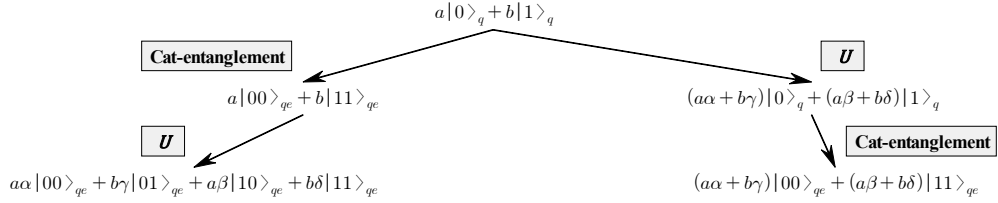


Fig. 21 A linked copy e of q is created at the module containing q' . The order of cat-entanglement and U matters.

Appendix C Derivation of (12)

In matrix representations,

$$\begin{aligned}
 \text{CP}_{12}(\theta) &= \begin{pmatrix} 1 & & & & & \\ & 1 & & & & \\ & & 1 & & & \\ & & & 1 & & \\ & & & & 1 & \\ & & & & & e^{i\theta} \\ & & & & & & e^{i\theta} \end{pmatrix} \\
 &= \begin{pmatrix} 1 & & & & & \\ & 1 & & & & \\ & & 1 & & & \\ & & & 1 & & \\ & & & & 1 & \\ & & & & & e^{i\theta} \\ & & & & & & e^{i\theta} \end{pmatrix} \begin{pmatrix} 1 & & & & & \\ & 1 & & & & \\ & & 1 & & & \\ & & & 1 & & \\ & & & & 1 & \\ & & & & & e^{i\theta} \\ & & & & & & e^{i\theta} \end{pmatrix} \begin{pmatrix} 1 & & & & & \\ & 1 & & & & \\ & & 1 & & & \\ & & & 1 & & \\ & & & & 1 & \\ & & & & & 1 \\ & & & & & & 1 \end{pmatrix} \\
 &= \text{SWAP}_{23} \text{CP}_{13}(\theta) \text{SWAP}_{23}.
 \end{aligned}$$

References

- Andres-Martinez, P., Forrer, T., Mills, D., Wu, J.-Y., Henaut, L., Yamamoto, K., . . . Duncan, R. (2024). Distributing circuits over heterogeneous, modular quantum computing network architectures. *Quantum Science and Technology*, 9(4), 045021,
- Andres-Martinez, P., & Heunen, C. (2019). Automated distribution of quantum circuits via hypergraph partitioning. *Physical Review A*, 100(3), 032308,
- Arute, F., Arya, K., Babbush, R., Bacon, D., Bardin, J.C., Barends, R., . . . others (2019). Quantum supremacy using a programmable superconducting processor. *Nature*, 574(7779), 505–510,
- Barenco, A., Bennett, C.H., Cleve, R., DiVincenzo, D.P., Margolus, N., Shor, P., . . . Weinfurter, H. (1995). Elementary gates for quantum computation. *Physical review A*, 52(5), 3457,
- Bourassa, J.E., Alexander, R.N., Vasmer, M., Patil, A., Tzitrin, I., Matsuura, T., . . . others (2021). Blueprint for a scalable photonic fault-tolerant quantum

- computer. *Quantum*, 5, 392,
- Bravyi, S., Gosset, D., König, R. (2018). Quantum advantage with shallow circuits. *Science*, 362(6412), 308–311,
- Cacciapuoti, A.S., Caleffi, M., Tafuri, F., Cataliotti, F.S., Gherardini, S., Bianchi, G. (2019). Quantum internet: Networking challenges in distributed quantum computing. *IEEE Network*, 34(1), 137–143,
- Cirac, J.I., Ekert, A., Huelga, S.F., Macchiavello, C. (1999). Distributed quantum computation over noisy channels. *Physical Review A*, 59(6), 4249,
- Clausen, J. (1999). Branch and bound algorithms-principles and examples. *Department of computer science, University of Copenhagen*, 1–30,
- Coppersmith, D. (2002). An approximate fourier transform useful in quantum factoring. *arXiv preprint quant-ph/0201067*, ,
- Cross, A.W., Bishop, L.S., Sheldon, S., Nation, P.D., Gambetta, J.M. (2019). Validating quantum computers using randomized model circuits. *Physical Review A*, 100(3), 032328,
- Cuomo, D., Caleffi, M., Krsulich, K., Tramonto, F., Agliardi, G., Prati, E., Cacciapuoti, A.S. (2023). Optimized compiler for distributed quantum computing. *ACM Transactions on Quantum Computing*, 4(2), 1–29,
- Draper, T.G. (2000). Addition on a quantum computer. *arXiv preprint quant-ph/0008033*, ,
- Eisert, J., Jacobs, K., Papadopoulos, P., Plenio, M.B. (2000). Optimal local implementation of nonlocal quantum gates. *Physical Review A*, 62(5), 052317,
- Ferrari, D., Carretta, S., Amoretti, M. (2023). A modular quantum compilation framework for distributed quantum computing. *IEEE Transactions on Quantum Engineering*, 4, 1–13,

- Fowler, A.G., Mariantoni, M., Martinis, J.M., Cleland, A.N. (2012). Surface codes: Towards practical large-scale quantum computation. *Physical Review A—Atomic, Molecular, and Optical Physics*, 86(3), 032324,
- G Sundaram, R., Gupta, H., Ramakrishnan, C. (2021). Efficient distribution of quantum circuits. *35th international symposium on distributed computing (disc 2021)* (pp. 41–1).
- Gurobi Optimization, LLC (2024). *Gurobi Optimizer Reference Manual*. Retrieved from <https://www.gurobi.com>
- Horowitz, M., & Grumblin, E. (2019). Quantum computing: progress and prospects.
- Karp, R.M. (2009). Reducibility among combinatorial problems. *50 years of integer programming 1958-2008: from the early years to the state-of-the-art* (pp. 219–241). Springer.
- Kjaergaard, M., Schwartz, M.E., Braumüller, J., Krantz, P., Wang, J.I.-J., Gustavsson, S., Oliver, W.D. (2020). Superconducting qubits: Current state of play. *Annual Review of Condensed Matter Physics*, 11(1), 369–395,
- Land, A.H., & Doig, A.G. (2009). An automatic method for solving discrete programming problems. *50 years of integer programming 1958-2008: From the early years to the state-of-the-art* (pp. 105–132). Springer.
- Neill, C., Roushan, P., Kechedzhi, K., Boixo, S., Isakov, S.V., Smelyanskiy, V., ... others (2018). A blueprint for demonstrating quantum supremacy with superconducting qubits. *Science*, 360(6385), 195–199,
- Nielsen, M.A., & Chuang, I.L. (2010). *Quantum computation and quantum information*. Cambridge university press.
- O’Malley, P.J., Babbush, R., Kivlichan, I.D., Romero, J., McClean, J.R., Barends, R., ... others (2016). Scalable quantum simulation of molecular energies. *Physical Review X*, 6(3), 031007,
- Papadimitriou, C.H., & Steiglitz, K. (1998). *Combinatorial optimization: algorithms and complexity*. Courier Corporation.
- Ruiz-Perez, L., & Garcia-Escartin, J.C. (2017). Quantum arithmetic with the quantum fourier transform. *Quantum Information Processing*, 16, 1–14,

- Sych, D., & Leuchs, G. (2009). A complete basis of generalized bell states. *New Journal of Physics*, 11(1), 013006,
- Terhal, B.M. (2015). Quantum error correction for quantum memories. *Reviews of Modern Physics*, 87(2), 307–346,
- Weinstein, Y.S., Pravia, M., Fortunato, E., Lloyd, S., Cory, D.G. (2001). Implementation of the quantum fourier transform. *Physical review letters*, 86(9), 1889,
- Wolsey, L.A. (2020). *Integer programming*. John Wiley & Sons.
- Wu, J.-Y., Matsui, K., Forrer, T., Soeda, A., Andrés-Martínez, P., Mills, D., . . . Murao, M. (2023). Entanglement-efficient bipartite-distributed quantum computing. *Quantum*, 7, 1196,
- Yimsiriwattana, A., & Lomonaco Jr, S.J. (2004). Generalized ghz states and distributed quantum computing. *arXiv preprint quant-ph/0402148*, ,
- Zaman, F., Jeong, Y., Shin, H. (2018). Counterfactual bell-state analysis. *Scientific reports*, 8(1), 14641,